Ultra-low power sensor for autonomous non-invasive voltage measurement in IoT solutions for energy efficiency

This is the post peer-review accepted manuscript of:

Clemente Villani, Domenico Balsamo, Davide Brunelli, Luca Benini, "Ultra-low power sensor for autonomous non-invasive voltage measurement in IoT solutions for energy efficiency," Proc. SPIE 9517, Smart Sensors, Actuators, and MEMS VII; and Cyber Physical Systems, 95172I (21 May 2015).

DOI: https://doi.org/10.1117/12.2181332

Ultra-low power sensor for autonomous non-invasive voltage measurement in IoT solutions for energy efficiency

Clemente Villani*[a], Domenico Balsamo[a], Davide Brunelli[b], Luca Benini[a,c]
[a]DEI, University of Bologna, viale Risorgimento 2, Bologna, Italy
[b]University of Trento, via Sommarive 9, Trento, Italy
[c]IIS, ETHZ, Gloriastrasse 35, Zurich, Switzerland

ABSTRACT

Monitoring current and voltage waveforms is fundamental to assess the power consumption of a system and to improve its energy efficiency. In this paper we present a smart meter for power consumption which does not need any electrical contact with the load or its conductors, and which can measure both current and voltage. Power metering becomes easier and safer and it is also self-sustainable because an energy harvesting module based on inductive coupling powers the entire device from the output of the current sensor. A low cost 32-bit wireless CPU architecture is used for data filtering and processing, while a wireless transceiver sends data via the IEEE 802.15.4 standard. We describe in detail the innovative contact-less voltage measurement system, which is based on capacitive coupling and on an algorithm that exploits two pre-processing channels. The system self-calibrates to perform precise measurements regardless the cable type. Experimental results demonstrate accuracy in comparison with commercial high-cost instruments, showing negligible deviations.

Keywords: Wireless Sensor Networks, Smart Metering, Energy Harvesting, contact-less voltage sensor, Non-Intrusive Load Monitoring.

1. INTRODUCTION

Nowadays the energy demand is constantly increasing from industrial, commercial and domestic customers. At the same time, the primary energy resources are going to exhaustion while the exploitation of renewable energy sources is not widespread enough to sustain the growing consumption [1]. In addition, the sub-optimal quality of the power supply transmission and an irresponsible usage of the electrical energy determine waste of energy and low reliability of distribution systems.
The efforts of the scientific community have been increased in recent years in the field of electrical energy management, and have been oriented to design new and smart ways to produce, to distribute and to use the energy. Smart Grids aims at the integration of ICT into the power grid to improve the efficiency, reliability, economics, and sustainability of the production and distribution of electricity [2].
At the consumer side, Smart Metering solutions are proposed to enable pervasive monitoring of energy consumption, to reduce waste and to analyze trends and behaviors. Making users aware of the energy consumption in their daily activities, fundamental for energy efficiency, needs distributed, low-cost, easy-to-use sensing systems, which monitor the power consumption of household's appliances [3].
In such a context, low-cost, unobtrusive and autonomous meters, which can harvest energy from their environment, play a key role. Indeed next-generation measurement systems must feature a small form factor, must be non-invasive and easy to install, and must be cost-effective in terms of production and maintenance [4]. The analysis of voltage and current waveforms for estimating energy consumption and power factor requires non-intrusive sensors, which can easily be installed in any circumstances, and the capability of converting energy from the surrounding environment becomes a strict requirement to reduce costs of battery replacement. In addition, smart meters may provide Non-intrusive Load Monitoring (NILM) techniques for disaggregating global energy consumption data in a household scenario [5-6].

In this paper we introduce a non-intrusive and self-sustainable wireless sensor node for smart metering applications, that uses clamp-on sensors for both current measurement and energy harvesting, and exploits new voltage contact-less sensor, based on capacitive coupling, which permits to measure the electrical potential between two conductors in a single-phase power line. The main objective is to obtain an easy-to-install device which does not need any breaking of the high-voltage AC power supply and is fully-autonomous, thanks to the energy harvesting subsystem. Moreover, the

*clemente.villani@studio.unibo.it; phone +39 051 2093837; fax +39 051 2093839; www-micrel.deis.unibo.it

node is capable of self-calibrating, that means it measures current and voltage waveform regardless the size and the insulator around the cables. Finally, the proposed smart sensor node is also low-cost: its performance in terms of measurement accuracy are comparable to those obtained with professional (and intrusive) measurement instruments.
The paper is organized as follows: Section 2 presents an overview of the non-intrusive measurement systems. Section 3 shows a description of the implementation of the proposed smart sensor node with a focus on the designed non-intrusive voltage measurement system. In Section 4, we discuss the experimental results, while Section 5 concludes the paper.

2. RELATED WORKS

The measurement of current through the magnetic field across a single wire is a well-established technique, using transducers such as Rogowsky coils, current transformers or Hall effect sensors [7-9]. Conversely, there is no commercially available non-invasive sensor which can measure the 230 AC voltage in wires for single-phase lines. Several solutions proposed in literature focus on monitoring in Extra/High-Voltage (EHV/HV) power systems. For example, the authors in [10] present a method to measure the voltage based on a capacitive system, but the monitored voltages are of the order of hundreds of kV. The authors in [11] propose a new resin-molded sensor for voltage and current monitoring. This sensor measures power consumption, power factor and harmonics in 6.6KV power line systems. Recently some solutions for Low-Voltage power system have been proposed, but none of them is suitable for our purpose. For example, the authors in [12] present a sensor with two capacitive probes for low-voltage systems to detect the voltage on a conductor without making direct contact with it. Nevertheless, the proposed sensor is not conceived to be used in voltage monitoring of cylindrical conductors, such as wires or cables, but for conductors with planar surfaces. Finally, the authors in [13] present a single sensor capable of measuring both the current and the voltage on a type of cable for domestic applications, but, due to the particular materials and production processes used to realize it, the cost is remarkably high, and, most of all, the sensor is suitable for only one type of cables.
In this paper we propose a non-invasive method for measuring the Low-Voltage (230-400V) waveform between the two wires of a single-phase power line. The proposed approach does not require interruption of power supply nor any breaking of the mains, which makes measurements much safer and easy, and includes an algorithm for self-calibrating, thus making the system suitable for all types of cables for household applications, as presented more in detail in the next section.

3. SYSTEM DESCRIPTION

The contribution of this paper is to enhance the Wireless Sensor Network node presented in [14-15] to achieve a complete non-intrusive and self-sustainable power meter, capable of sensing in a contactless manner also the voltage waveform of a single-phase electrical loads independently of type of cable, in addition to the current waveform, as the previous version, and calculating the power features of the electric load: power factor, apparent power, active power and reactive power.

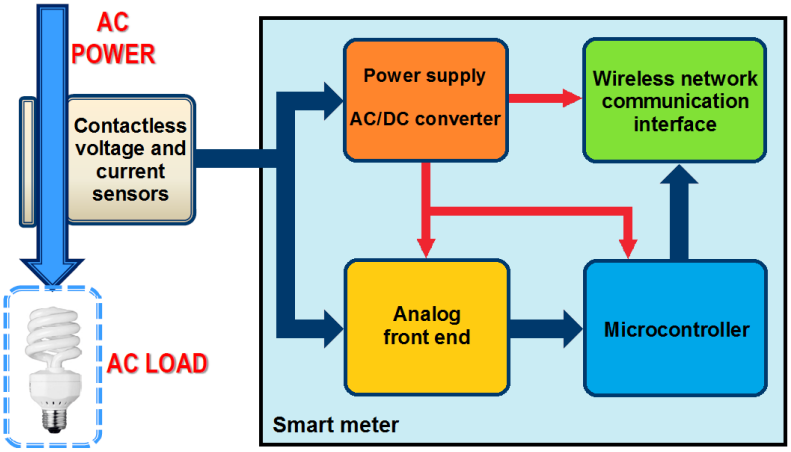

Figure 1. Schematic view of the proposed smart meter with the main blocks that compose it.

A schematic view of the proposed smart meter is shown in Figure 1, and it consists of these blocks: the contactless voltage and current sensors, connected to the energy harvesting system (that supplies the whole node) and to the analog front end. Finally, the microcontroller computes the measurement data and send it to the local central gateway through the wireless module. Each meter exploits a clamp-on transformer for current measurement and energy harvesting, and a new non-invasive capacitive-coupling sensor for voltage measurement.
In the following subsections, we describe the four parts that compose the meter architecture: i) the microcontroller and wireless transceiver, ii) the current sensing section, iii) the energy harvester, iv) the voltage sensing section.

A – Microcontroller and Wireless Transceiver

Our architecture is based on the JN5148 module from NXP, which provides an ultra-low power, high performance wireless microcontroller targeted to WSN applications, a 512kB serial flash memory and a real-time clock. The microcontroller features an enhanced 32-bit RISC processor, a 2.4GHz IEEE 802.15.4 compliant radio transceiver, 128kB ROM, 128kB RAM, and a complete set of analogue and digital peripherals such as a 12-bit ADC, a 12-bit DAC, a SPI interface etc. The key features of the JN5148 module are the very low sleep current, only 2.6µA, and the low power consumption of the radio transceiver (namely at 3.0V it draws 15mA during transmission and 17.5mA when receiving).
The smart meter transmits data to the Energy@Home compliant Gateway [16] (connected to a java-enabled host), using ZigBee PRO protocol with Home Automation profile. This gateway is a commercial product called FlexKey and it is one of the most compact Zigbee USB Dongle available on the market today. Due to its RF performance, it enables secure and reliable wireless connectivity between internal and external environment.

B – Current sensing section

To convert current to voltage we used a clamp-on current transformer. This sensor performs a non-intrusive measurement, based on the magnetic field across the wire, so it does not require any interruption or cutting of wires and it is much easier and safe to install. The adopted current transformer features linear performance over a wide range of input currents. Its main electrical characteristics are the number of turns (n=3000) and the maximum input current of 60A, which corresponds to a maximum input current of 20mA.

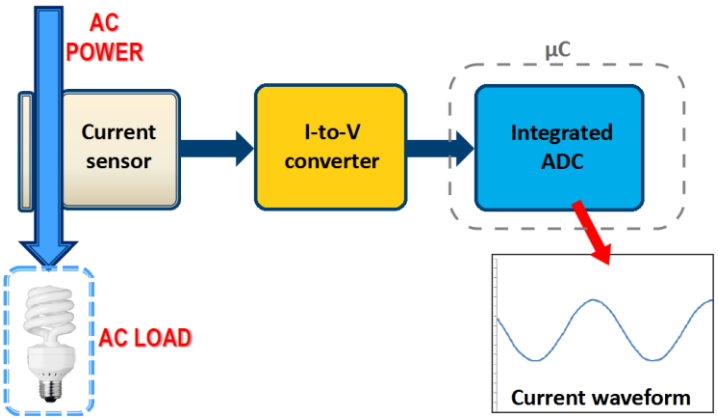

Figure 2. Block diagram of the current sensing circuit.

Figure 2 shows the block diagram for the current measurement. The current coming from the inductive coupling is converted to a proportional voltage, which is then sampled by the MCU ADC and elaborated by the 32-bit microcontroller.

C – Energy harvester

The energy harvesting circuit shares the same current transformer used for the current measurement as power transducer. When the node is in sleep mode, the energy harvesting system charges the supercapacitor that makes for energy buffer, recovering the energy lost during the active mode, in which the transformer is used for sensing current. Using the supercapacitor, the smart meter perform a start-up without any external energy storage. Figure 3 shows the block diagram of the system used to switch from the current measurement circuit to the energy harvesting system. The system starts executing the association with the Energy@Home compliant gateway only when the supercapacitor has enough charge.

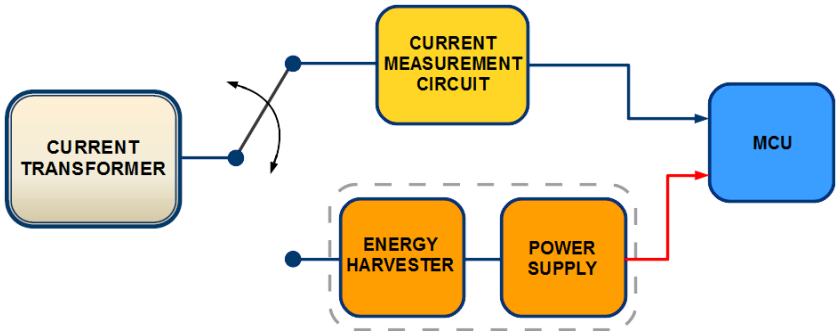

Figure 3. Block diagram of the switching system between the current sensing circuit and the energy harvesting system.

D – Voltage sensing section

The knowledge of the voltage waveform is important for measuring the Power Factor (PF), that is the ratio between the real power P (measured in W) and the apparent power |S| (measured in VA, where S is the complex power, measured in VA and given by the sum of active power P and reactive power Q, measured in var). PF spans from 0 to 1, but international regulations suggest to keep it bigger than 0.9 using dedicated compensation circuits. It is important to note that the PF value measures not just the contribution of the phase lag ϕ between voltage and current, but also the high frequency content of the input current. This harmonic content, as well as the phase lag ϕ, is regulated by the European Standard EN 60555, which defines the limits and the constraints for appliances and mains.
In the following subsections, we present the innovative non-intrusive and self-calibrating system we designed for electrical potential difference measurement.

D.1 – Voltage sensors:

The voltage sensors is based on capacitive coupling: we put a cylindrical conductor of length l=1.25cm around the cable, as shown in Figure 4.

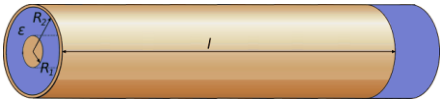

Figure 4. Block diagram of the switching system between current sensing circuit.

In this way, we obtain a cylindrical capacitor consisting in the internal conductor of the wire, of radius R1, and the external hollow conductor, of radius R2, separated by the insulating of the cable, with permittivity ε. The capacitance between the two conductors of such structure is given by the formula:

$$C = \frac{2\pi l \varepsilon}{\ln \frac{R_1}{R_2}} \qquad (1)$$

Considering a normal cable for domestic applications, with R1=2÷3mm, R2=3÷4mm, and a PVC insulator, C accounts from some pF, as evaluated from the equation (1).

Applying this sensor on both cables of the power lines, we obtain the differential input of our system, as shown in Figure 5a, which is equivalent to model the input voltage between the terminal of two capacitors as shown in the scheme of Figure 5b.

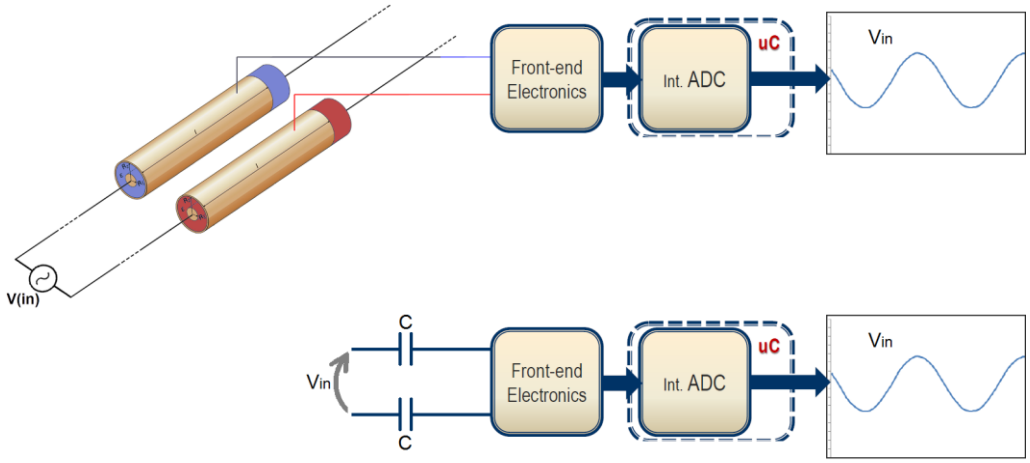

Figure 5. a) Block diagram of the voltage measurement system. b) Equivalent circuit for the analog front-end input.

D.2 – Mathematical model:

The problem statement consists of equations which permit to calculate two unknown variables (i.e., the capacitance C and the voltage V_{in}). These two equations are given by the transfer functions of the two analog filters we chose to realize the analog processing front end.

One of these two filters is shown in Figure 6. It is an impedance voltage divider, made of two capacitances: the input unknown capacitance C and a capacitance C_1 of 6.8nF, whose optimal value has been estimated through simulations, in order to discern even smaller values of the input voltage and not to exceed the microcontroller ADC maximum sampling value.

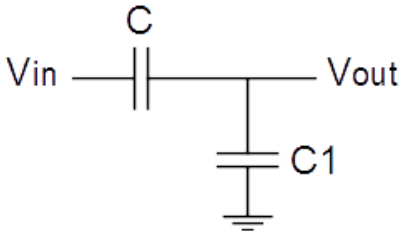

Figure 6. The first of the two filters used to implement the mathematical two-equation system that models the problem.

The input-output relationship of this CC filter is:

$$V_{outCC} = \frac{C}{C + C_1} V_{in} \tag{2}$$

This is a real function, so it just attenuates V_{in} by a certain values dependent by the input capacitance C, without modifying its phase.

The second filter is shown in figure 7. It is a high-pass filter made of a voltage divider with two resistances (R_1 of 1 GΩ, and R_2 of 3MΩ) in series to the input capacitance. The resistance values are calculated with the aim of maximize the span and optimize the accuracy of each power range too.

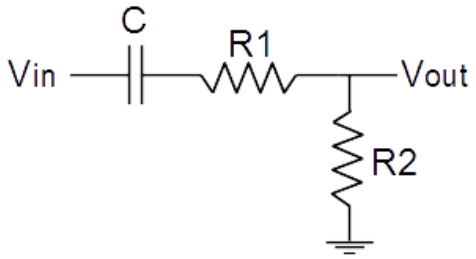

Figure 7. The second filter used to implement the mathematical system.

The transfer function of this CRR filter is:

$$H_{CRR}(s) = \frac{V_{outCRR}}{V_{in}} = \frac{sCR_2}{1 + sC(R_1 + R_2)} \tag{3}$$

The cut-off frequency of this filter is given by:

$$f_t = \frac{1}{2\pi C(R_1 + R_2)} \tag{4}$$

From the transfer function, the resulting module and phase of the frequency response of this filter are given by:

$$\left|H_{CRR}(j\omega)\right| = \frac{\omega CR_2}{\sqrt{1 + \omega^2 C^2 (R_1 + R_2)^2}} \tag{5}$$

$$\varphi_{CRR} = \tan^{-1}\left[\frac{1}{\omega C(R_1 + R_2)}\right] \tag{6}$$

So, starting from the phase ϕ_{CRR}, that is the phase shift corresponding to the delay between the V_{outCC} waveform (that is in phase with V_{in}) and the V_{outCRR} waveform (that is shifted of ϕ_{CRR} from Vin and, therefore, from V_{outCC}), we can obtain the value of the input capacitance C reversing the (6), and then the waveform of V_{in}, reversing the (2).

D.3 – The analog front end:

Figure 8 shows the complete analog front end we have designed for the voltage measurement system.

Each input channel is connected to accomplish both the CC filter and the CRR filter through a MCU-controlled switch, used to select the filter. Every filter output is decoupled from downstream circuit with a buffer. Then we used an OPAMP in differential configuration to send a differential signal to the ADC. Finally, to avoid waste of energy, all OPAMPs can be turned off when not working, with a MCU-controlled pMOS which enables/disables their power supply. We also introduced a reference voltage (generated from the supply voltage) in the common mode node of filters and OPAMPs to bias their output voltages to positive values and therefore get the system works correctly in the negative semi-period of input signal too.

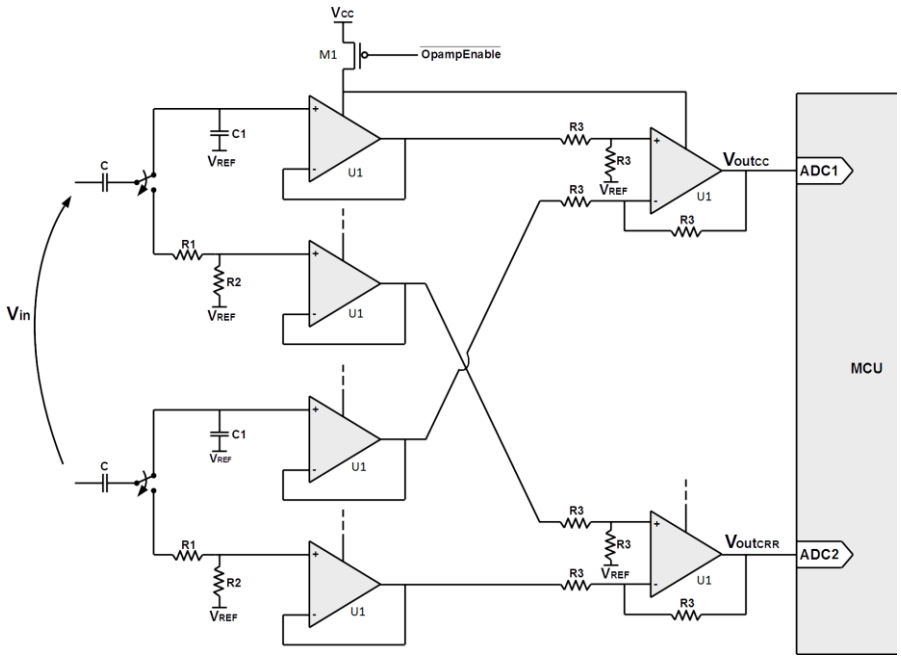

Figure 8. The analog front-end circuit of the designed contact-less voltage measurement system.

D.4 – Voltage measurement algorithm:

The following steps summarize the algorithm designed to implement voltage measurement:

i. when the node wakes up from the sleep mode, it samples a period of V_{outCC} and then a period of V_{outCRR} (paying attention to start the second sampling after a multiple of signal period from the beginning of sampling of V_{outCC});

ii. measures the delay between V_{outCC} and V_{outCRR}, and converts this time in an angle (considering that a delay of a whole period corresponds to a phase shift of 360°), obtaining ϕCRR;

iii. reversing the (6), calculates C, with the formula:

$$C = \frac{1}{2\pi f\left(R_1 + R_2\right)\tan\left(\varphi_{CRR}\right)} \tag{7}$$

iv. reversing the (2), calculates V_{in} waveform from V_{outCC} waveform, with the formula:

$$V_{in} = \left(1 + \frac{C_1}{C}\right)V_{outCC} \tag{8}$$

D.5 – Power features calculation:

The described algorithm produces the factor $\left(1 + \frac{C_1}{C}\right)$, that lets us calculate the desired power features sampling several periods of the current signal and of V_{outCC}, which, multiplied for that factor gives the V_{in} signal.
From these arrays of samples, we can get the root mean square values for input current and voltage, using the formulas:

$$V_{RMS} = \sqrt{\frac{1}{N}\sum_{k=0}^{N-1} v^2[k]} \quad ; \quad I_{RMS} = \sqrt{\frac{1}{N}\sum_{k=0}^{N-1} i^2[k]} \tag{9; 10}$$

Hence, we can calculate the apparent power |S| with the following:

$$|S| = V_{RMS} \cdot I_{RMS} \tag{11}$$

We can also calculate the active power P directly from the instantaneous powers p[k]:

$$P = \frac{1}{N}\sum_{k=0}^{N-1} p[k] = \frac{1}{N}\sum_{k=0}^{N-1} v[k]\, i[k] \tag{12}$$

As the active power P can be also written with the following:

$$P = V_{RMS} \cdot I_{RMS} \cdot PF \tag{13}$$

hence, we can calculate the power factor PF as:

$$PF = \frac{P}{|S|} \tag{14}$$

Finally, we can calculate the absolute value of the reactive power Q with the following:

$$Q = |S|\sqrt{1 - PF^2} \tag{15}$$

4. EXPERIMENTAL RESULTS

All tests were realized with the highest ADC sampling frequency for the JN5148 microcontroller, 100KHz, and with a sleep time for the sensor node of 60 seconds. The cables used for the tests include all the main types of wires for domestic applications and are listed in Table 1, while in Figure 9 is shown the prototype of the smart metering system used to realize the tests.

Table 1. Properties of the types of cable for domestic applications used for the tests.

Cable external section diameter (mm)	Cable internal section diameter (mm)	Capacitance (pF)
8.0	5.5	12
6.0	4.0	11
4.5	3.0	10
3.5	2.0	9
3.0	1.5	8
2.5	1.5	8

Results for Power Factor measurement, reported for three types of cables, are shown in Table 2, in which they are compared with the values measured with an intrusive power meter. For each cable, different values of loads are used. Measured values demonstrate the performance of the proposed non-intrusive measurement system in comparison to professional instruments.

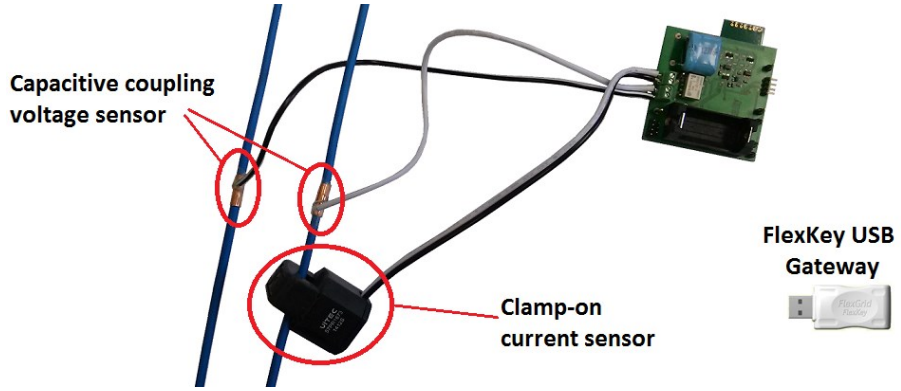

Figure 9. Contact-less smart power meter prototype.

Table 2. Results for PF measurement for three types of cables, compared with the intrusive power meter measurements.

		PF measured with the non-intrusive smart meter	PF measured with the intrusive power meter	Error from the intrusive power meter (in %)	Deviation from non-intrusive smart meter average value (in %)
Cable with C=12pF	Load 1	0.9981	1.000	0.19	0.05007
		0.9987	1.000	0.13	0.01001
		0.9990	1.000	0.10	0.04006
	Load2	0.9981	0.780	1.01	0.25874
		0.7841	0.780	0.53	0.22480
		0.7856	0.780	0.72	0.03393
	Load 3	0.9981	0.610	0.98	0.40750
		0.6106	0.610	0.10	0.47270
		0.6139	0.610	0.64	0.06520
	Load4	0.9981	0.490	0.92	0.16152
		0.4939	0.490	0.80	0.28266
		0.4975	0.490	1.53	0.44418
Cable with C=10pF	Load 1	0.9985	1.000	0.15	0.00668
		0.9982	1.000	0.18	0.02337
		0.9986	1.000	0.14	0.01669
	Load 2	0.8019	0.800	0.24	0.05401
		0.8003	0.800	0.04	0.25343
		0.8048	0.800	0.60	0.30744
	Load 3	0.6186	0.610	1.41	0.25390
		0.6169	0.610	1.13	0.02161
		0.6156	0.610	0.92	0.23229
	Load4	0.4789	0.470	1.89	0.22323
		0.4769	0.470	1.47	0.19533
		0.4777	0.470	1.64	0.23229
Cable with C=8pF	Load 1	0.9974	1.000	0.26	0.01671
		0.9982	1.000	0.18	0.06349
		0.9971	1.000	0.29	0.04678
	Load 2	0.7979	0.800	0.26	0.04176
		0.7978	0.800	0.28	0.05429
		0.7990	0.800	0.13	0.09605
	Load3	0.6526	0.650	0.40	0.23441
		0.6540	0.650	0.62	0.02038
		0.6558	0.650	0.89	0.25479
	Load 4	0.4955	0.490	1.12	0.28844
		0.4979	0.490	1.61	0.19453
		0.4974	0.490	1.51	0.09391

As can be noted, PF values measured with the proposed non-intrusive smart meter has an error from the values measured with the intrusive power meter lower than 2% and a deviation from the measured average value for a fixed load lower than 0.5%.

Results for voltage measurement, reported for three types of cables, are shown in Table 3, compared with the values measured with an intrusive power meter. The error for the voltage measurement is negligible too, in fact it is lower than 3%, as can be seen in the table.

Table 3. Results for voltage measurement for three types of cables, compared with the intrusive power meter measurements.

		Voltage measured with the non-intrusive smart meter	Voltage measured with the intrusive power meter	Error (in %)
Cable with C=12pF	Load 1	224.2	224.3	0.05
	Load 2	222.3	226.5	1.85
	Load 3	221.3	225.5	1.86
Cable with C=10pF	Load 1	229.6	224.3	2.36
	Load 2	230.4	226.5	1.72
	Load 3	231.4	225.5	2.62
Cable with C=8pF	Load 1	228.5	224.3	1.87
	Load 2	228.8	226.5	1.02
	Load 3	229.8	225.5	1.91

5. CONCLUSIONS

In this paper we present a wireless sensor node for smart metering, compliant to IEEE 802.15.4 standard, focusing on an innovative non-intrusive manner to measure the voltage waveform in a single-phase electrical line, and computing power consumption features together with the current consumption. It exploits contact-less sensors both for current and for voltage signal, making the node easy to install and the measures much safer. The proposed system is also energetically self-sustainable, thanks to an energy harvest module, which shares the current sensor used for current measuring. The achieved accuracy is high, in fact the average error for the electrical parameter measurement (i.e., current and voltage waveforms, power features) is lower than 3%. Hence, results are comparable to professional (and intrusive) measurement instruments, but at a cost that is dozens of times lower.

ACKNOWLEDGMENT

The research contribution presented in this paper has been supported by a research grant from Telecom Italia, by the project FLEXMETER (grant no:646568) funded by the EU H2020 Framework Programme, and by the ARTEMIS Innovation Pilot Project: ARROWHEAD (grant no: 332987) funded by the ARTEMIS Joint Undertaking.

REFERENCES

[1] “Earth Overshoot Day.” [Online]. Available: http://www.footprintnetwork.org/en/index.php/GFN/page/earth_overshoot_day

[2] S. M. Amin and B. Wollenberg, “Toward a smart grid: power delivery for the 21st century,” IEEE Power and Energy Magazine, 2005, vol. 3, pp. 34–41, Sept - Oct 2005.

[3] S. Ahmad, “Smart metering and home automation solutions for the next decade,” in Proc. of the international conference on Emerging Trends in Networks and Computer Communications, 2011 (ETNCC 2011), Apr 22-24 2011, pp. 200–204.

[4] S. Depuru, L. Wang, V. Devabhaktuni, and N. Gudi, “Smart meters for power grid, challenges, issues, advantages and status,” Power Systems Conference and Exposition (PSCE), 2011 IEEE/PES, march 2011.

[5] J. Liang, S. K. Ng, G. Kendall, and J. W. Cheng, “Load signature study - part 1: Basic concept, structure, and methodology,” Power Delivery, IEEE Transactions on, vol. 25, no. 2, pp. 551–560, April 2010.

[6] J. Liang, S. K. Ng, G. Kendall, John W.M., and Cheng, “Load signature study - part 2: Disaggregation framework, simulation, and applications,” Power Delivery, IEEE Transactions on, vol. 25, no. 2, pp. 561–569, April 2010.
[7] P. Ripka, “Electric current sensor: A review,” Meas. Sci. Technol., vol. 21, no. 11, pp. 112001-1–112001-23, Nov. 2010.
[8] S. Ziegler, R. C. Woodward, H. H. Iu, and L. J. Borle, “Electric current sensors: A review,” IEEE Sensors J., vol. 9, no. 4, pp. 354–376, Apr. 2009.
[9] C. Xiao, “An overview of integratable current sensor technologies,” in Conf. Rec. IEEE 38th IAS Annu. Meeting, Salt Lake City, UT, USA, Oct. 2003, vol. 2, pp. 1251–1258.
[10] L. Wu, P. Wouters, E. van Heesch, and E. Steennis, “On-site voltage measurement with capacitive sensors on high voltage systems,” in PowerTech, 2011 IEEE Trondheim, 2011, pp. 1–6.
[11] T. Kubo, T. Furukawa, H. Fukumoto, and M. Ohchi, “Numerical estimation of characteristics of voltage-current sensor of resin molded type for 22kv power distribution systems,” in ICCAS-SICE, 2009, pp. 5050–5054.
[12] K. Tsang and W. Chan, “Dual capacitive sensors for non-contact ac voltage measurement,” Sensors and Actuators A: Physical, vol. 167, no. 2, pp. 261–266, 2011.
[13] Y. Chen, W. Hsu, S. Cheng, and Y. Cheng, “A Power Sensor Tag With Interference Reduction for Electricity Monitoring of Two-Wire Household Appliances,” IEEE Transactions on Industrial Electronics, vol. 61, no. 4, pp. 2062-2070, 2014.
[14] D. Porcarelli, D. Balsamo, D. Brunelli, and G. Paci, “Perpetual and lowcost power meter for monitoring residential and industrial appliances,” in Design, Automation Test in Europe Conference Exhibition, 2013, pp. 1155–1160.
[15] D. Balsamo, D. Porcarelli, D. Brunelli, and L. Benini, “A new non-invasive voltage measurement method for wireless analysis of electrical parameters and power quality,” IEEE, 2013.
[16] “Energy@home.” [Online]. Available: ”http://www.energy-home.it”